



Fabrication of zein-based electrospun nanofiber decorated with gold nanoparticles as a SERS platform

Hazal Turasan¹ , Mukerrem Cakmak² , and Jozef Kokini^{1,*} 

¹Department of Food Science, Purdue University, 745 Agriculture Mall Nelson Hall, West Lafayette, IN 47907, USA

²School of Materials and Mechanical Engineering, Purdue University, 1205 W. State St, West Lafayette, IN 47907, USA

Received: 2 December 2018

Accepted: 4 March 2019

Published online:

18 March 2019

© Springer Science+Business Media, LLC, part of Springer Nature 2019

ABSTRACT

In this study, a new technique was developed to create an eco-friendly and biodegradable SERS sensor platform using electrospun corn zein fibers. First, electrospinning was used in conjunction with glutaraldehyde, a crosslinker for proteins, to create crosslinked zein nanofibers. The surface of the nanofibers was then decorated with 20-nm-diameter gold nanoparticles, and the biosensor platform was tested with the Raman active Rhodamine 6G. The high surface area and the high surface roughness enabled a SERS signal enhancement of 1.06×10^6 , which only required 2.8×10^{-7} g of gold nanoparticle deposition on the fibers. This electrospun zein-based gold nanoparticle-decorated sensor platform is not only made with a quicker, simpler and an inexpensive method compared to the other techniques requiring etching procedures and has a very good shelf life stability, but also serves as a green alternative to the plastic-based SERS sensor platforms with an equivalent and sometimes lesser SERS signal enhancement.

Introduction

The advantages of biosensors, such as their rapid detection, specificity, ease of mass fabrication, economics and point-of-care applicability, make them useful and preferred diagnostic techniques for medicine, environmental monitoring, food safety/quality and agricultural applications [1]. Extensive studies have been carried out focusing on fabricating sensors in the literature [2–4]. Surface-enhanced Raman spectroscopy (SERS) is a sensor technique aiming to enhance the intensity of scattering obtained from the

Raman active molecules by using noble metal nanoparticles and nanostructures which facilitate the formation of hot spots. SERS is a rapid technique, and it only takes minutes and sometimes just seconds to make the measurements. The availability of portable, handheld Raman devices makes point-of-care (on-site) measurements possible and practical [5].

The exponentially increasing number of sensors, being used to detect various molecules, brings up the concern for the amount of plastics and synthetic materials used for the production of these biosensors. Therefore, there is a need for more eco-friendly “green” biosensors. Some of the examples where

Address correspondence to E-mail: jkokini@purdue.edu

sensors are fabricated using eco-friendly materials include a chitosan-based biosensor and a zein-based biosensor [6, 7]. Despite their advantages, using these food-grade polymers in the fabrication of biosensors has considerable challenges; for example, there may be a need for the addition of a non-biodegradable filler or polymer to have the similar properties as a synthetic material (plastic)-based sensor leading to fabrication methods that are very time- and resource-consuming. For example, for the fabrication of chitosan-based biosensors, the addition of nanocomposites (laponite [8] or graphene [6]) was necessary to increase the electro-catalytical activity of the chitosan films. The fabrication of SERS biosensors necessitates the incorporation of small amounts of highly dispersed noble metal components like gold or silver. For example, in the fabrication of zein (corn protein)-based SERS biosensor, the process includes master mold preparation, PDMS curing and solvent evaporation. Also a 200-nm layer of gold coating was necessary to get a SERS enhancement of $\sim 10^4$ [7]. In applications like these, producing the biodegradable sensor defeats its purpose.

Electrospinning is a technique which enables the fabrication of nanoscale fibers using different polymeric substrates [9, 10]. It may be possible that the large surface area created during the fabrication of these fibers may lead to an alternative design for SERS sensors. Therefore, in this study, we benefit from the high surface area created by electrospinning and from the biodegradability of a waste corn protein, zein, by producing electrospun zein nanofibers. The design parameters for the fabrication of zein nanofibers have been explored in depth [11–15]. In a detailed study, the dependence of fiber morphology on the viscosity and the concentration of zein solutions were carefully analyzed [13]. The critical entanglement concentration (C_e) of zein in 80% aqueous ethanol solution was found as 12 wt %, and for the fabrication of beadless fibers, the minimum zein concentration was calculated as $2\text{--}2.5C_e$ (25 wt %). At viscosities lower than 100 mPa s, the entanglement of zein molecules was not enough to create bead-free fibers, but at higher viscosities increasing chain entanglements were high enough to facilitate beadless fibers [13]. A more recent study, where pristine and blend (with PEO) zein fibers were fabricated from 80% ethanol solution, confirmed these findings [15]. The C_e of zein was found as 11.2 wt%, and the minimum zein concentration for the

fabrication of bead-free fibers was similarly twice as much as C_e (22 wt%). The specific concentration of zein, where the surface tension of the solution changed from the solvent's surface tension to zein monolayer surface tension, was found as 22 wt%, further confirming the minimum necessary zein concentration for bead-free fiber formation [12]. Studies of bead-free zein fiber formation using other solvents showed slightly different concentration windows (> 27 wt% for acetic acid, > 35 wt% for DMF) possibly due to different behaviors of zein in these solvents [14]. For the fabrication of zein fibers in our study, we have studied concentrations above the reported critical concentrations.

In this study, electrospinning is used to create a new zein-based SERS biosensor platform. We aim to benefit from the increasing surface area of zein when fibers are fabricated. We hypothesize that increased surface area would enable a more effective gold deposition on the surface of zein, which would help to obtain SERS intensity enhancement higher than the previously developed zein film-based SERS platform [7]. We also aim to significantly reduce the amount of noble metal used in the fabrication of the zein-based biosensor platform to preserve the biodegradability of the biosensor.

Materials and methods

Materials

Zein powder was obtained from Sigma-Aldrich. Ethanol, glacial acetic acid, glutaraldehyde (GLA) aqueous solution (25%) and Rhodamine 6G were purchased from Fisher Scientific. Gold (Au) nanoparticles (20 nm) were purchased from Ted Pella Inc. (Redding, CA) at a concentration of 7.0×10^{11} particles ml^{-1} .

Solution preparation

Zein solutions were prepared by dissolving zein powder in glacial acetic acid at ratios of 26 wt%, 28 wt% and 30 wt%. To prepare the solutions for the electrospinning process, they were stirred for 2 h at 50 °C and cooled down to room temperature.

For crosslinked zein fibers, zein solutions were crosslinked with glutaraldehyde (GLA). Prior studies have shown that zein films crosslinked with GLA at a

concentration of 12 wt% of the amount of zein were the strongest films and gave the highest number of crosslinks [16]. Therefore, in this study, the relative amount of GLA was also set at 12 wt% of the amount of zein used to prepare the solutions. For instance, to prepare a solution with 6.5 g zein, 3.12 g aqueous GLA solution, which contained 0.78 g GLA, was measured in a beaker and was left under the fume hood overnight for the water to evaporate prior to zein solution preparation. After water evaporation, zein and acetic acid were added to the same beaker to reach a final zein concentration of 26 wt% for the 26% zein sample. Similar calculations were made for the 28% and 30% solutions. The solutions with all the necessary ingredients were stirred similar to the uncrosslinked solutions.

Electrospinning

The zein solutions were electrospun at 20 kV using a high voltage power supply (Lambda Electronics). The distance between the needle and the collecting plate was fixed at 10 cm, and the collecting plate was covered with aluminum foil for high conductance and ease of handling. The two dispensing tip types (inner diameters 0.635 mm (JG20-0.5X) and 0.381 mm (JG24-0.5X)) were purchased from Jensen Global Inc. A syringe pump (Pump Systems Inc.) was used to supply 5 in.H₂O pressure and a flow rate of 0.86 ml/h. Electrospinning was performed at 20% relative humidity (room relative humidity) and at 22 °C. During the collection of the zein fibers, glass slides were placed underneath the spinneret for collection of the fibers for optical microscopy imaging and Raman measurements. Due to the fast evaporation of the solvent at the nozzle caused by the very high surface area generated by electrospinning, occasional blockage of the zein solution stream occurred. In those cases, the power supply was turned off and the tip of the needle was cleaned, and the system was started again. After the electrospun fibers were collected on the aluminum sheets or glass slides, the samples were kept in desiccators for further drying.

To manufacture fibers using crosslinked zein with glutaraldehyde, the fibers exiting the spinneret were collected as before but additionally were subjected to heat to accelerate the crosslinking process in a conventional oven at 140 °C for 10 min following a previously developed method [17]. After they were taken out of the oven, these fibers were also stored at

the desiccators containing Drierite (W.A. Hammond Drierite Co., LTD).

To compare the effect of heat on uncrosslinked zein fiber properties, a batch of uncrosslinked zein fibers was also similarly heated at 140 °C. These samples were then used to compare the water contact angles (WCA) of the zein mats without crosslinking with those with crosslinking following the WCA methodology described in “[Water contact angle measurements](#)” section.

This is important in the SERS platform design of the fibers because when water droplets containing gold nanoparticles are deposited on the surface, it is highly desirable for the droplet not to spread so that gold nanoparticles are concentrated in one small spot. Therefore, the more hydrophobic the surface can be made, the less the spreading of the droplet will occur. The samples prepared here enable the comparison of this relevant and important surface property.

Optical microscopy imaging

An optical microscope (Olympus BX51) was used to image the zein nanofibers collected on the glass slides during electrospinning at 10× magnification.

EDX to detect gold nanoparticles and scanning electron microscopy to study micro- and nanostructure and confirm and augment data obtained with EDX

Nova NanoSEM 200 Scanning Electron Microscopy was used for SEM imaging of the samples collected on the aluminum foil (used to ensure conductance). 1 cm × 1 cm squares were cut from aluminum foils covered with fibers and coated with a platinum/palladium mixture for 60 s (Cressington 208 HR sputter coater). The images were collected with an accelerating voltage of 5.0 kV and at a working distance ranging between 3.8 and 5.6 mm. The images were collected at varying magnifications.

To see the distribution of the gold nanoparticles on zein nanofibers, first, energy-dispersive X-ray analysis (EDX) was done. However, for some of the zein nanofiber mats, the gold nanoparticles are distributed on the nanofibers as individual particles (away from each other) instead of aggregating. This separate distribution of gold nanoparticles on the surface is mostly seen on the uncrosslinked zein nanofiber

mats, where spreading of the drop of gold nanoparticle solution to a wider area separated the gold nanoparticles from each other and prevented aggregation. Because the size of the nanoparticles (20 nm diameter) is lower than the pixel size of EDX mapping, especially in low magnification (wider area) images, EDX maps did not show significant peaks of individual gold nanoparticles, and most of the information was lost during EDX mapping for uncrosslinked fibers.

Instead of EDX mapping, SEM images of the samples taken with a backscattered electron detector (vCD) displayed the distribution of gold nanoparticles on the nanofibers more accurately, because in backscattered electron detection, gold nanoparticles can be easily spotted and differentiated from platinum/palladium (used to cover the surface of the sample for conductivity) due to their higher atomic number. This higher atomic number makes the gold nanoparticles shine more brightly than platinum during backscattered electron imaging.

Gold nanoparticle decoration of the electrospun zein fibers

The zein nanofibers were decorated with 20-nm gold nanoparticles using two different methods. No crosslinker was used in either of the decoration methods. In the first method, the nanoparticle colloids were added into the zein solutions before the electrospinning step. After the solutions were cooled down to room temperature, 60 μl of the gold colloid solution (7.0×10^{11} particles ml^{-1}) was added to 10 ml of zein solution and stirred for another 15 min to ensure homogenous distribution. Then, the solutions were electrospun as described in “[Electrospinning](#)” section.

In the second way of nanoparticle decoration, 2 μl droplets of nanoparticle colloids (7.0×10^{11} particles ml^{-1}) were deposited on the dried electrospun zein fiber mats. The fiber mats were then placed in desiccators containing desiccant (W.A. Hammond Drierite Co., LTD) to ensure the complete drying of the colloids. To further enhance the concentration of gold nanoparticles, multiple droplet deposition was used. Multiples of 2 μl droplets (3 consecutive droplets) were placed on the same spot on the fibers with drying periods in between, such that the new droplets were placed on the same spot after the previous droplet has dried.

Water contact angle measurements

Water contact angle measurements were conducted on zein fiber mats electrospun directly onto glass slides using Attension Theta Tensiometer (Biolin Scientific). The contact angles were recorded for 50 s with 12 frames per second. The droplet size of the water placed on each sample was 2 μl . Right and left contact angles were averaged by the software. The initial average contact angles ($t = 0$ s) and contact angles at 5 s, 10 s and 50 s were reported.

Degradation in aqueous environment

To test the stability of both uncrosslinked and cross-linked electrospun zein nanofibers in aqueous environment, water immersion test was conducted. 1 cm \times 1 cm pieces of zein nanofiber mats, which were directly electrospun on aluminum foil, were immersed in 15 ml deionized water in 60 mm \times 15 mm petri dishes for 30 min. To ensure complete immersion in water, the samples were taped to the bottom of the petri dishes. After 30 min of immersion, the samples were dried in an oven at 120 $^{\circ}\text{C}$ for 1 h to evaporate the water for SEM imaging. SEM images were taken with the parameters explained in “[EDX to detect gold nanoparticles and scanning electron microscopy to study micro- and nanostructure and confirm and augment data obtained with EDX](#)” section.

Atomic force microscopy

Cypher ES Atomic Force Microscopy from Asylum Research was used to characterize the surface roughness of the electrospun fiber mats. TAP300AL-G-10 type silicon probes coated with 30 nm Al for enhanced reflectivity (tip radius < 10 nm) with 300 kHz frequency and 40 N m^{-1} force constant were purchased from Ted Pella Company. AFM analysis was conducted on the zein fibers electrospun directly on aluminum sheets. 0.5 cm \times 0.5 cm pieces were cut from the fiber-coated aluminum sheets and superglued on AFM/STM Metal Specimen Discs. The images were taken from 10 $\mu\text{m} \times 10 \mu\text{m}$ and 300 nm \times 300 nm scanning areas. The average roughness values were calculated by MFP3D software.

Raman spectroscopy measurements

Raman spectroscopy was conducted on zein nanofibers with a dispersive Raman spectrometer (DXR 2 Raman Microscope ThermoFisher Scientific). The spectra were collected between wavenumbers of 200 and 3600 cm^{-1} using a 633-nm laser at 6 mW laser power, 10x objective lens with a 50 μm slit aperture. Ten replications were taken for each spectrum and averaged using OMNIC software. Due to the fluorescence of zein protein, the baseline of all the spectra was initially corrected for fluorescence using fifth-order polynomial. Then, all the spectra were manually fine-tuned for baseline correction. The Raman active Rhodamine 6G (R6G) was used as a Raman marker. First, electrospun zein nanofiber mats were decorated with Au nanoparticles using two consecutive droplets of 2 μl (7.0×10^{11} particles. ml^{-1}). Then, a third droplet of 2 μl , containing 1 μl Rhodamine 6G (200 μM) mixed with 1- μl Au nanoparticles (7.0×10^{11} particles. ml^{-1}), was deposited on the zein nanofibers prior to Raman measurements, giving a final Rhodamine 6G concentration of 100 μM . The electrospun zein fiber mats were then put into desiccators for complete evaporation of the solvent. The measurements were taken after the Rhodamine 6G solvent evaporated.

Statistical analysis

Minitab 18 (one-way ANOVA) was used for statistical analyses with 95% confidence level. Tukey's comparison tests were applied ($p < 0.05$) to compare the zein fiber diameters and the water contact angle data. Lettering system was used to show significant difference, such that different letters represent significant difference.

Results and discussions

In this paper, we report the design and optimization of zein fiber mat fabrication for the best possible Au nanoparticle decoration to obtain a higher SERS enhancement than what has previously been reported [7]. Effects of solvent, zein concentration, crosslinking and nanoparticle decoration methods have been studied to obtain fibers with smaller diameters and the highest resistance to swelling. Smaller diameters are important to get the highest

possible surface area to enable more particle decoration, and resistance to swelling is important for Au colloid and sample depositions. The optimized fibers were then tested for SERS measurements to calculate the enhancement factor.

Effect of solvent on fiber morphology

In this study 70% ethanol and glacial acetic acid were tested as the solvents for the fabrication of zein fiber mats in terms of their suitability for SERS sensors because they are known as the two best solvents for zein [18]. Figure 1 shows the optical microscopy images of zein fibers prepared from these two solvents at 26 wt%. When 70% ethanol was used as the solvent, there were a lot of inhomogeneity and discontinuities in the fibers in the form of beads, which led to frequent fiber rupture and discontinuous fiber formation (Fig. 1a). The fibers fabricated using glacial acetic acid were largely bead-free, and there were almost no fiber breakages (Fig. 1b), consistent with the previous studies [14, 17].

The different morphologies of zein fibers in 70% ethanol and glacial acetic acid are due to different chain entanglement behaviors of zein molecules in these solvents as explained in introduction. The incomplete unfolding of zein molecules in ethanol solutions leads to multimer formation of zein molecules through hydrophobic interactions [12]. Clearly, at this concentration of zein in 70% ethanol, the lack of interaction between zein multimers does not allow enough chain entanglement between zein molecules to provide the continuity of the macromolecular phase in solution during electrospinning, which leads to bead formation and fiber rupture [19]. Even though the zein concentration used in this study for 70% ethanol (26 wt%) was above the reported critical entanglement concentrations (22–25 wt%) [13, 15], beaded fibers were still observed, which is probably due to different sources of zein used and the small variations in the solubility of zein at this ethanol concentration in the solvent. In the case of acetic acid, zein molecules have been shown to better and fully dissolve and unfold, leading to only monomer formation in the solvent [12]. This complete unfolding of zein molecules at the same concentration allows more chain entanglement of zein molecules in acetic acid solution, which leads to a continuous fiber formation during solvent evaporation. A schematic

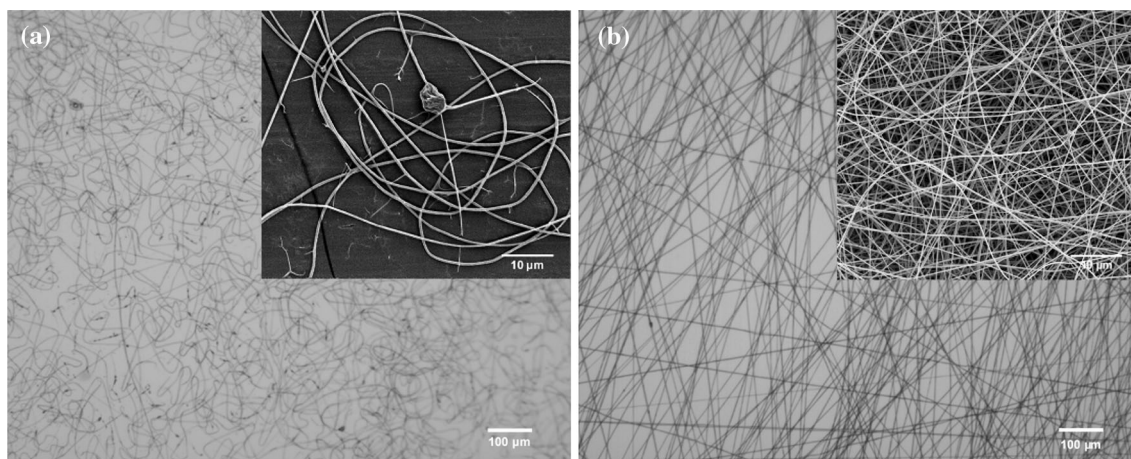


Figure 1 Optical microscopy images (at 10x magnification) of zein electrospun fibers prepared using 70% ethanol solution (a) and glacial acetic acid (b) as solvents. Corresponding SEM images are given as insets.

representation of zein fiber formations in aqueous ethanol and in acetic acid is shown in Fig. 2.

Because fabricating zein fibers using acetic acid as the solvent resulted in continuous fiber formation with significantly less defects and preparing fibers from 70% aqueous ethanol solution caused frequent bead formation and fiber breakages, for the rest of the experiments, only acetic acid was used as the solvent.

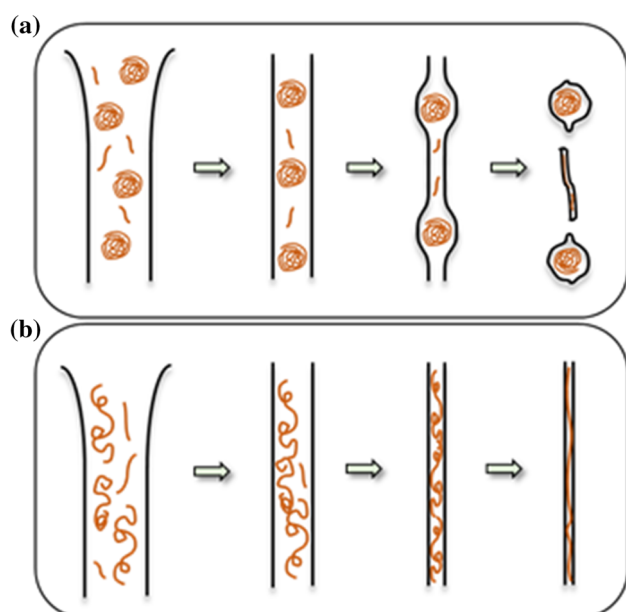


Figure 2 Schematic representation of electrospun zein fiber formation using 70% aqueous ethanol (a) and glacial acetic acid (b) as solvent.

Effect of zein concentration on fiber morphology

Three different zein concentrations (26 wt%, 28 wt% and 30 wt%) were tested to fabricate fibers, and their behaviors under aqueous media deposition were studied (section “[Decoration of zein fibers with gold nanoparticles](#)”). In the fabrication of zein fiber-based SERS biosensor platforms, decreasing fiber diameter would result in increased surface area, which would also increase the number of gold nanoparticles that can be deposited/decorated on the surface of zein, leading to an increase in hot spot formation and therefore an increased SERS signal. The fibers need to have resistance to swelling leading to limited swelling when aqueous samples are applied on them to keep their 3D structures. Initially, all three zein solutions were electrospun using a dispensing tip having an inner diameter of 0.381 mm. However, the solution prepared with 30 wt% zein could not be drawn out due to its higher viscosity (2.0 Pa.s) and dispensing tips with an inner diameter of 0.635 mm were used. The viscosity of the solutions that have 26 wt% and 28 wt% zein concentrations was low enough to use dispensing tips with 0.381 inner diameter (0.8 Pa s and 1.3 Pa s, respectively) and at the same time high enough to be above the critical concentration ($2C_e$) for entanglement to successfully manufacture fibers (Online Resource 1 for viscosity measurements).

Zein fibers were successfully fabricated from all three concentrations as shown in SEM images in Fig. 3. All the fibers had smooth surfaces without

cracks. In almost all of the fibers, the cores of the fibers are darker compared to the walls possibly because of the shrinking during drying that may result in a somewhat higher concentration in the middle compared to the walls. However, this shrinkage did not prevent the fibers from having round shapes. Almost no fusion of the fibers was observed at the junction points, which shows that zein fibers are drying efficiently before being collected on the collecting plate without causing any fusion. The fibers with highest zein concentration (30 wt%) had the highest average diameter (830 ± 156 nm) as expected based on prior studies of the electrospinning of zein, followed by 28 wt% zein fibers with an average diameter of 312 ± 66 nm and 26 wt% zein with an average diameter of 289 ± 63 nm [20]. Statistical analysis (ANOVA)

showed that while fibers with 30 wt% zein had significantly larger diameters, fibers with 26 and 28 wt% were not significantly different from each other.

Our results are consistent with previous studies where round and beadless zein fibers were fabricated using zein in the concentration range (27–30 wt%) in glacial acetic acid as the solvent [14, 21]. Lower concentrations of zein caused electrospinning instead of electrospinning. In this study, zein fibers were successfully fabricated with a good geometry with 26 wt% zein. This difference may be due to using dispensing tips with different inner diameters.

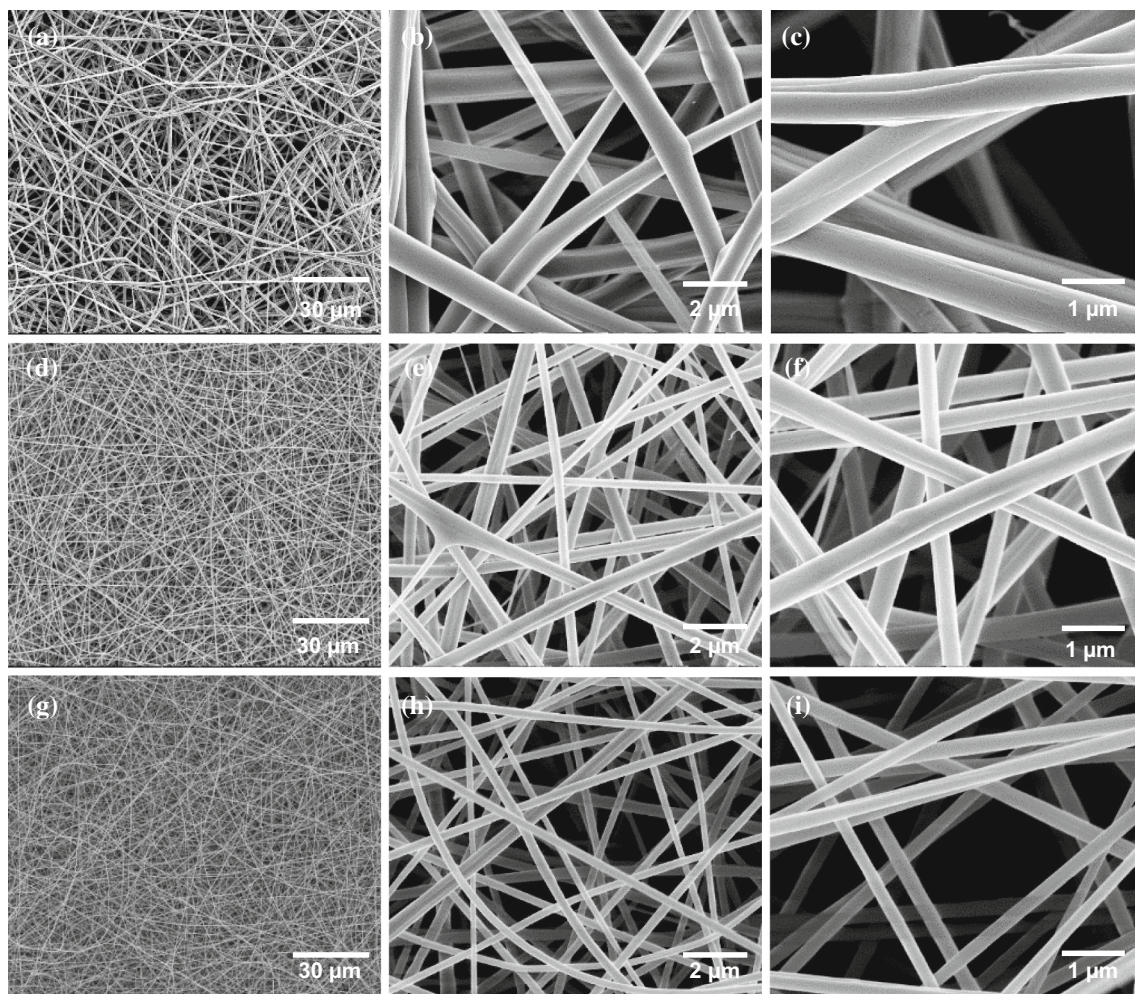


Figure 3 SEM images of zein nanofibers with a–c 30 wt%, d–f 28 wt% and g–i 26 wt% zein concentration at different magnifications (a, d, g at 2000 \times , b, e, h at 25,000 \times and c, f, i at 50,000 \times).

Decoration of zein fibers with gold nanoparticles

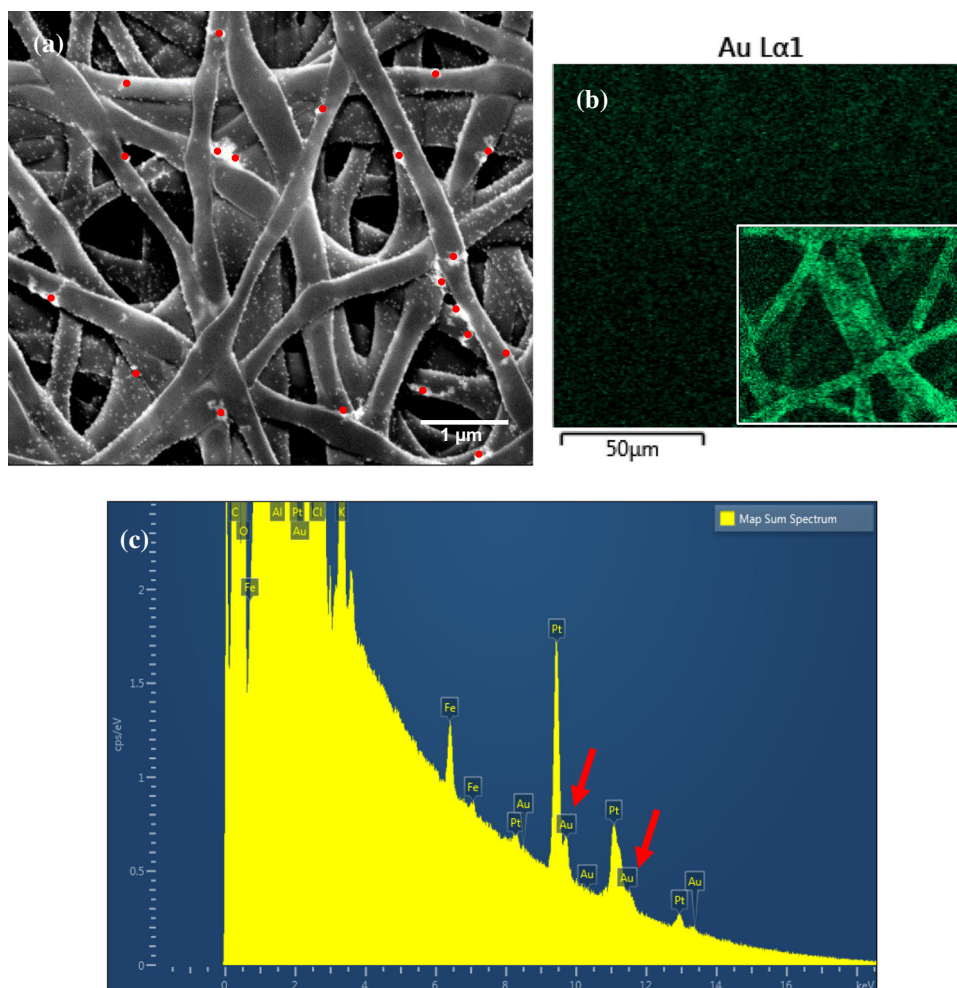
EDX analysis versus backscattered electron (BSE) imaging

To display the distribution of gold nanoparticles, EDX and BSE imaging techniques were compared as explained in “EDX to detect gold nanoparticles and scanning electron microscopy to study micro- and nanostructure and confirm and augment data obtained with EDX” section. An example of poor mapping of gold nanoparticles with EDX analysis is shown below. Figure 4a shows the SEM image of an uncrosslinked zein nanofiber mat decorated with 3 consecutive droplets (2 μl each) of Au nanoparticles taken using a backscattered electron detector (vCD) at high magnification (gold nanoparticles are highlighted artificially with red dots). Figure 4b, c shows the Au EDX map and EDX map spectrum of the same sample, respectively. The EDX map (Fig. 4b) does not

show the accurate distribution of the nanoparticles on the fiber structure, but instead it shows a background signal distribution. For comparison, an EDX map of a crosslinked zein nanofiber mat showing a more accurate distribution gold nanoparticles is shown in the inset of Fig. 4b. However, this accurate nanoparticle distribution could not be captured for uncrosslinked samples. Also in Fig. 4c, the Au peaks have low intensities in the spectra and are mostly hidden in the background signal. This also shows that correct information could not be obtained from all of our samples using EDX mapping.

Instead of EDX mapping, SEM images of the samples taken with a backscattered electron detector (vCD) displayed the distribution of gold nanoparticles on the nanofibers more accurately. In backscattered electron detection, gold nanoparticles can be easily spotted and differentiated from platinum due to their higher atomic number. This higher atomic number providing more electrons makes the gold

Figure 4 BSE image (a), Au EDX map (b), and EDX map spectrum (c) of uncrosslinked zein nanofiber decorated with Au nanoparticles. Inset in b shows Au EDX map of crosslinked zein nanofiber decorated with Au nanoparticles.



nanoparticles shine more brightly than platinum during backscattered electron imaging. Figure 5a shows the difference between two areas on the fiber mats decorated and non-decorated with Au nanoparticles imaged with backscattered electron detector. Both of these areas were covered with platinum before imaging. It is clear that brightness comes only from gold and not from platinum. EDX analysis of the crosslinked fiber mats with no platinum cover but only with gold nanoparticle decoration (Fig b) also proves that the brightness is due to the distribution of gold nanoparticles and not platinum (Fig c). Therefore, to better show the distribution of the gold nanoparticles on zein nanofibers, backscattered electron imaging was conducted instead of EDX mapping.

In-solution method

In this technique 20-nm Au nanoparticles were used as explained in section “[Gold nanoparticle decoration](#)

[of the electrospun zein fibers.](#)” The SEM images of the zein nanofibers decorated with “in-solution” method are shown in Fig. 6. All the fibers have similar morphologies to those of control nanofibers. All the samples had quite smooth surfaces. Occasionally some cracks formed caused by the high energy of SEM imaging. In almost none of the fibers, nanoparticles were seen on the surface of the fibers. This is possibly due to fast drying of nanofibers, which ended up encapsulating the gold nanoparticles in the interior region of the fibers. Au nanoparticles were very rarely seen during SEM imaging (data not shown), especially around broken fibers, which were probably surfaced by diffusing to the surface through the cracks. SEM image of 26 wt% zein nanofibers taken with a backscattered electron (BSE) detector also proves that there are no gold nanoparticles on the surface of the nanofibers decorated with “in-solution” decoration method, since there are no distinctive brighter spots in the image (Fig. 6d). It was concluded that as far as SERS application was

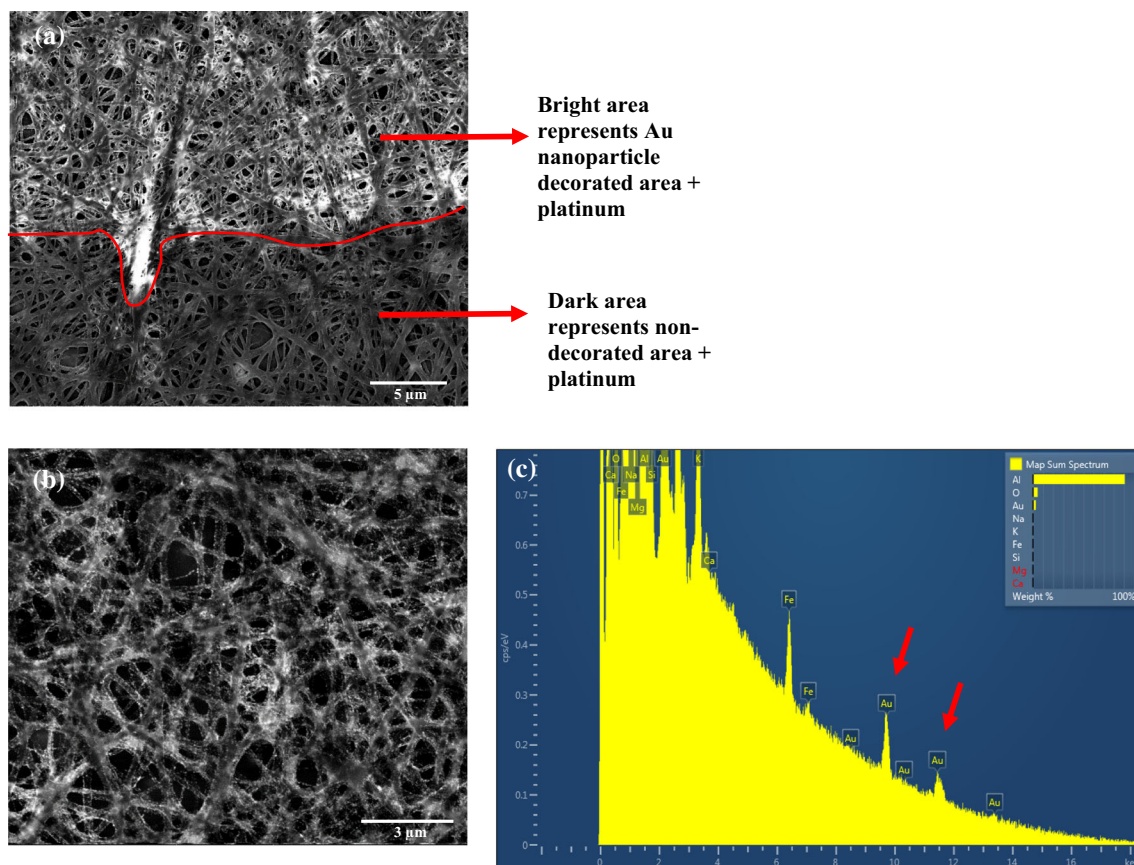
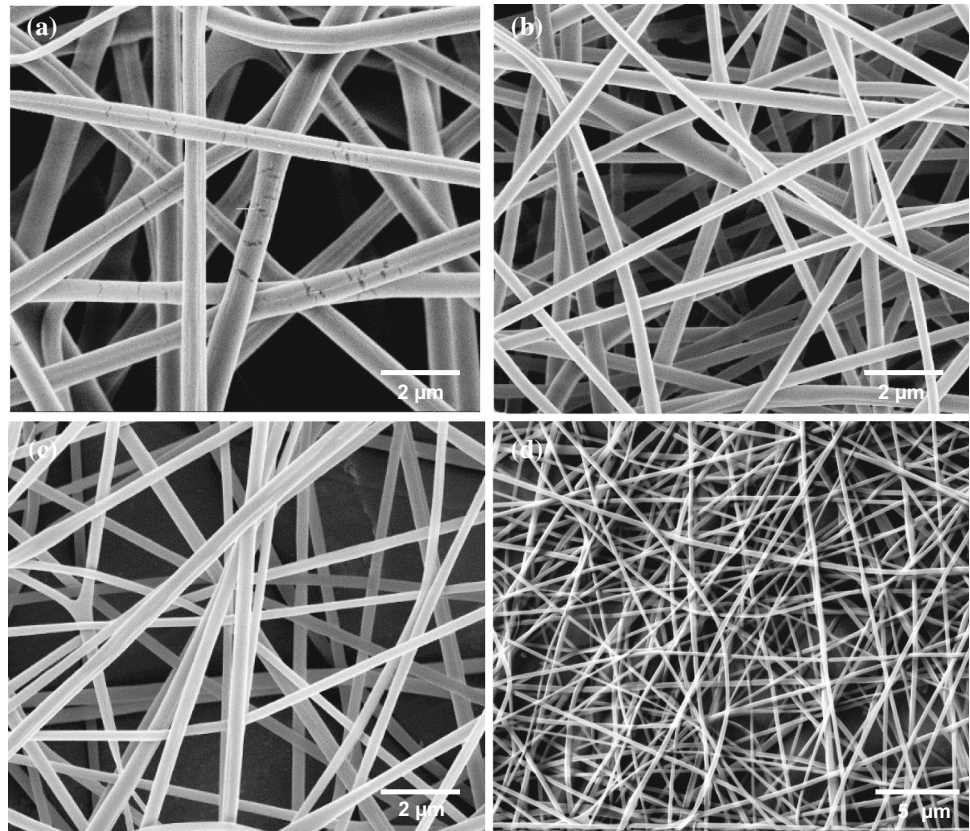


Figure 5 BSE image of crosslinked zein nanofibers decorated with Au nanoparticles coated with platinum/palladium for imaging (a). BSE image (b) and EDX map spectrum (c) of uncoated crosslinked zein nanofibers decorated with Au nanoparticles.

Figure 6 SEM images of zein nanofibers decorated with gold nanoparticles using “in-solution” method having 30 wt% (a), 28 wt% (b), and 26 wt% (c) zein concentrations. SEM image of 26 wt% zein nanofibers taken with a BSE detector (d).



concerned, this was not a successful method and as a result was not pursued any further.

Drop deposition method

Zein nanofibers decorated with the drop deposition technique show some similarities and some differences in morphology to those decorated with the “in-solution” method as shown in Fig. 7a–c. At the junction points where the fibers cross after electrospinning, there are some distortions and some fibers merge, possibly due to localized absorption of water and swelling coming from the liquid drop. The general structure of the fibers is nevertheless well preserved (Fig. 7a–c). The gold colloid filled droplet deposition does not seem to change the surface smoothness of the fibers compared to the control fibers. Fibers fabricated from a solution of 30 wt% zein seem to be less distorted compared to 28 wt% or 26 wt% zein fibers at single drop deposition. During solvent evaporation of the drop, the water may not be able to diffuse deep into the 30 wt% fibers compared to the fibers with lower zein concentrations because the diameter of the fibers fabricated from 30% zein

solution is considerable larger than the fibers from 26 and 28% zein solutions.

The nanoparticle concentration is kept constant for all the fibers (7×10^{11} particles ml^{-1}). However, for all the nanofibers, at some places the nanoparticles are aggregating while at other places they are better dispersed on the surface (Fig. 7a–c). Aggregation of nanoparticles is seen more around the intersection of nanofibers. It would be expected that as the liquid from the droplet is being absorbed into the fiber mat through capillary action, the gold nanoparticles would be attracted toward regions where there is an abundance of zein (intersections of fibers) given the proven affinity of gold to zein [7].

To test if increasing the number of gold nanoparticle droplets increases the nanoparticle density on the surface of the nanofibers, 2 and/or 3 consecutive droplets (each droplet having a 2 μl volume) were deposited on the same spot of the nanofiber mats. Between the depositions of two consecutive drops, the earlier gold colloid droplet was dried in the desiccator. This way, the liquid volume on that spot was not doubled or tripled at once, since it would cause further swelling and the gold nanoparticles

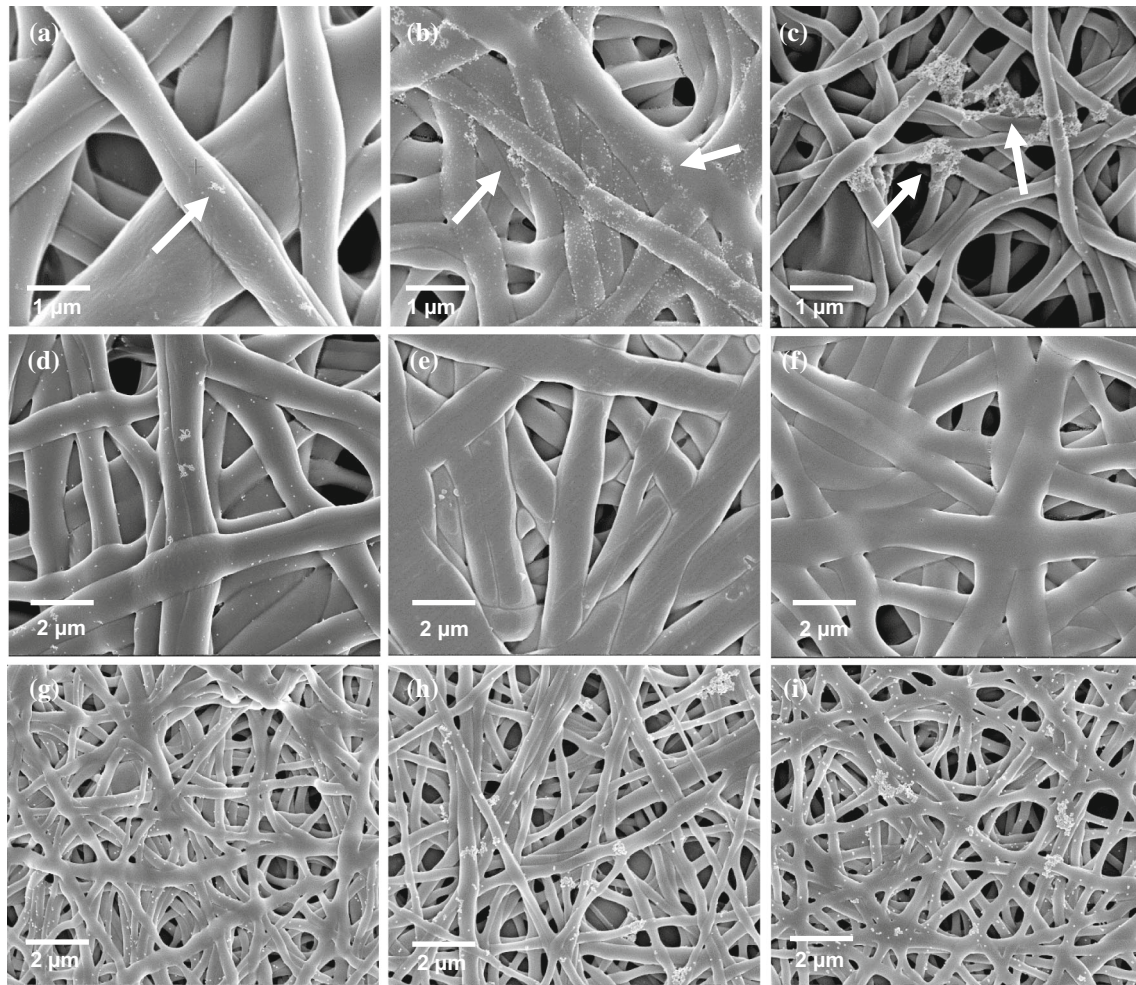


Figure 7 SEM images of zein nanofibers decorated with single drop deposition having 30 wt% (a), 28 wt% (b), and 26 wt% (c) zein concentrations. The arrows are showing the Au nanoparticle clusters on the surface of the nanofibers. Effect of

multiple Au colloid droplet deposition on 30 wt% (d–f) and 26 wt% (g–i) zein nanofibers (d, g: single droplet; e, h: two consecutive droplets; f, i: three consecutive droplets).

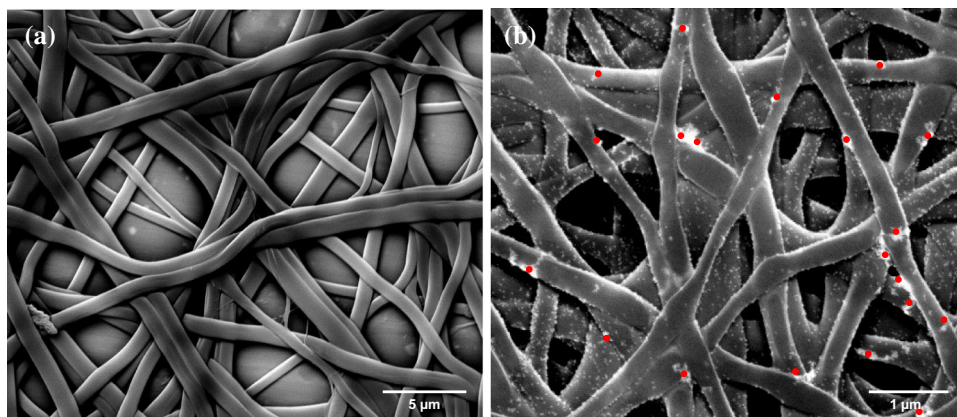
would spread themselves to a larger surface adversely affecting the Raman enhancement, but instead, the concentration of gold nanoparticles on the same spot of the mats was increased by applying 2 or 3 droplets consecutively once the spot dried. The number of Au nanoparticles was increased on the same spot with the goal of increasing the intensity of the Raman signal during SERS because the decrease in gold interparticle distance would enhance hot spot formation. Figure 7d–i shows the zein nanofiber mats with Au nanoparticles deposited on the surface with 1, 2 and 3 consecutive droplets.

To display the increasing concentration of gold nanoparticles decorated on the surface of the zein nanofibers with increasing number of gold colloid droplets, BSE images of 26 wt% zein nanofibers

decorated with 1 droplet and 3 droplets of gold nanoparticle colloid are shown in Fig. 8a, b, respectively. It is clear from the higher number of brighter spots seen on the fibers decorated with 3 droplets the concentration of gold nanoparticles increases significantly with multiple droplet deposition, which is favorable to increase the number of hot spots for enhancing the Raman signal.

The addition of 2 or 3 droplets sequentially further increased the swelling for the largest diameter fibers (30 wt% zein), but no significant increase in the surface density of gold nanoparticles was observed. The additional swelling also caused partial loss of 3D structure and the formation of a more planar structure (Fig. 7d–f).

Figure 8 Backscattered electron images of 26 wt% zein nanofibers decorated with 1 droplet (a), and 3 droplets (b) of gold nanoparticle colloid solution. Some of the gold nanoparticle dense spots are highlighted with red dots.



The 26 wt% fibers on the other hand, representing the smallest diameter fibers, did not further swell with more droplet deposition. The morphology of the fiber mats decorated with 2 droplets was very similar to those decorated with 3 droplets (Fig. 7g–i). Multiple droplet deposition was also helpful in increasing the number of Au nanoparticles on the surface of the fibers. For this reason, 26 wt% zein concentration was used further in this study to understand the effect of gold decorated fibers on SERS enhancement.

Effect of crosslinking on surface wettability of zein nanofibers

In this study, the effect of crosslinking of zein with glutaraldehyde on surface properties of the fiber mat was tested to determine if the surface would become progressively more hydrophobic in order to prevent the spreading of gold nanoparticle containing droplets so that the gold nanoparticles are assembled in a relatively small surface area to maximize the intensity of the SERS signal. The number of crosslinks in zein films increases with increasing glutaraldehyde concentration in the range of 0–12% glutaraldehyde with 12% giving the highest crosslink density [16]. Therefore, the nanofibers were crosslinked with glutaraldehyde at 12 wt% and heated at 140 °C for 10 min [17]. There were no visual differences between the crosslinked and uncrosslinked or heated and non-heated fiber mats. Also, there were no visible changes occurring in the sample morphology with heat treatment (Fig. 9). No visible contraction or collapse of the fibers was observed after heating the samples.

The surface wettability properties of the nanofiber mats, measured using the WCA, changed

significantly with both crosslinking and heat treatment. Table 1 shows the water contact angles of crosslinked and uncrosslinked zein nanofiber mats with and without heat treatment at different times.

As expected, the lowest initial contact angles were recorded for the uncrosslinked samples that were not subjected to any heat treatment. The absorption of the water droplet by the nanofiber mat was the fastest for this sample; 10 s after the droplet was placed on the nanofiber mat, the droplet was fully absorbed. 12% crosslinking increased the initial ($t = 0$) contact angle of the nanofiber mats; however, without extensive crosslinking, after 10 s the water droplet was again fully absorbed. The initial contact angle of the uncrosslinked fiber mats increased to 123°, and the absorption rate of the water droplet into the fiber matrix significantly decreased because of heat treatment at 140 °C. The slowest water droplet absorption and the highest initial contact angle were seen in the 12% crosslinked nanofiber mat subjected to heat treatment at 140 °C. The initial WCA rose to 134°, and even after 50 s, the water droplet was not fully absorbed caused by the combined effects of crosslinking and heat treatment. Consistent with our observations, previous studies have shown that forming electrospun fibers from a material increases its surface hydrophobicity, due to the increase in surface roughness both at the micro- and nanolevels, which is also known as the lotus effect [22–25]. In addition, crosslinking zein films with 12% glutaraldehyde also increases their surface roughness [16]. Additionally, heat treatment enhances chemical crosslinking, contributing to the surface roughness, and may help the evaporation of the bound hydrophilic solvent trapped inside the nanofibers, further increasing the surface hydrophobicity.

Figure 9 SEM images of 12% crosslinked zein fiber mats without (a) and with (b) 140 °C heat treatment for 10 min.

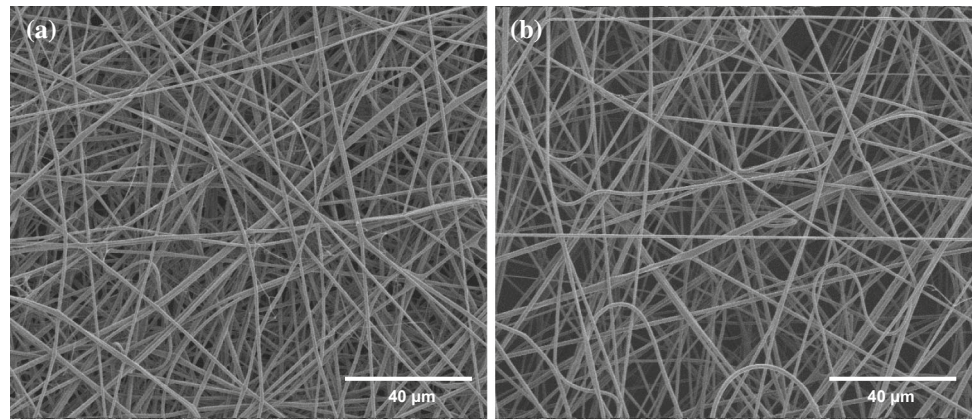


Table 1 Water contact angles of crosslinked and uncrosslinked zein nanofibers with and without heat treatment (each time period was statistically compared within itself, and different letters show significant difference, $p < 0.05$)

WCA	0% GLA non-heated (°)	12% GLA non-heated (°)	0% GLA heated at 140 °C (°)	12% GLA heated at 140 °C (°)
$t = 0$ s	57.34 ± 12.07^d	86.25 ± 4.76^c	123.19 ± 4.68^b	134.40 ± 3.25^a
$t = 5$ s	12.39 ± 3.30^c	16.81 ± 1.61^c	71.77 ± 6.64^b	115.20 ± 4.09^a
$t = 10$ s	0	0	17.78 ± 6.55^b	87.60 ± 18.20^a
$t = 50$ s	0	0	0	59.99 ± 18.59

The changing surface wettability, caused by the combined effects of crosslinking and heat treatment, had a significant effect on gold nanoparticle decoration of the nanofibers (Fig. 10a, b). For the uncrosslinked and non-heated nanofibers (Fig. 10a), the nanoparticles deposited on the surface of the fibers were located far apart from each other with the exception of a few clusters. This is due to the fast spreading of water through the gaps between fibers, which widened the area that Au nanoparticles were deposited on. Also, part of the gold nanoparticles are possibly dragged by water to the bottom of the nanofiber mats and lose their effectiveness in Raman signal amplification. The nanoparticles on the surface of the 12% crosslinked and heated nanofibers (Fig. 10b) are more densely populated. The increasing surface hydrophobicity prevented the spreading of the water carrying the gold nanoparticles, which resulted in a higher concentration of nanoparticles. Backscattered electron images of these nanofibers at lower magnifications show the increasing concentration of gold nanoparticles with crosslinking and heat treatment more clearly and effectively (Fig. 10c–d). Since higher concentrations and more clustering of the gold nanoparticles are expected to enhance hot spot formation during the SERS measurements, samples that are 12% crosslinked and heat treated were used in SERS experiments.

Degradation in aqueous environment and during storage in an average relative humidity environment

SEM images of uncrosslinked and crosslinked zein nanofibers before and after immersion in deionized water are shown in Fig. 11. For uncrosslinked zein nanofibers, even though there were a few fibrous structures seen after the water immersion test, most of the fiber morphology was lost. The swelling of zein nanofibers with water caused merging and flattening of the fibers, forming a film structure (Fig. 11c).

The crosslinked zein nanofibers maintained their fibrous structures against swelling much better than the uncrosslinked zein nanofibers. However, partial film formation due to swelling and merging was also seen in crosslinked zein nanofibers (Fig. 11d). This higher stability of crosslinked zein nanofibers in an aqueous environment is due to the stronger structure of zein created by tighter junctions during chemical crosslinking with glutaraldehyde [16].

However, the most relevant storage experiment are those that are conducted in an average relative humidity environment. We have stored crosslinked zein nanofibers in the relative humidity environment of our laboratory for 8 months. The results are shown in Fig. 11e. As can be seen from the figure, fibers

Figure 10 Combined effects of crosslinking and heat treatment on nanoparticle decoration. SEM images of uncrosslinked non-heated (a) and 12% crosslinked and heated (b) zein nanofibers decorated with 20-nm Au nanoparticles. BSE images of uncrosslinked non-heated (c) and 12% crosslinked and heated (d) zein nanofibers decorated with 20-nm Au nanoparticles. Some of the gold nanoparticle dense spots are highlighted with red dots.

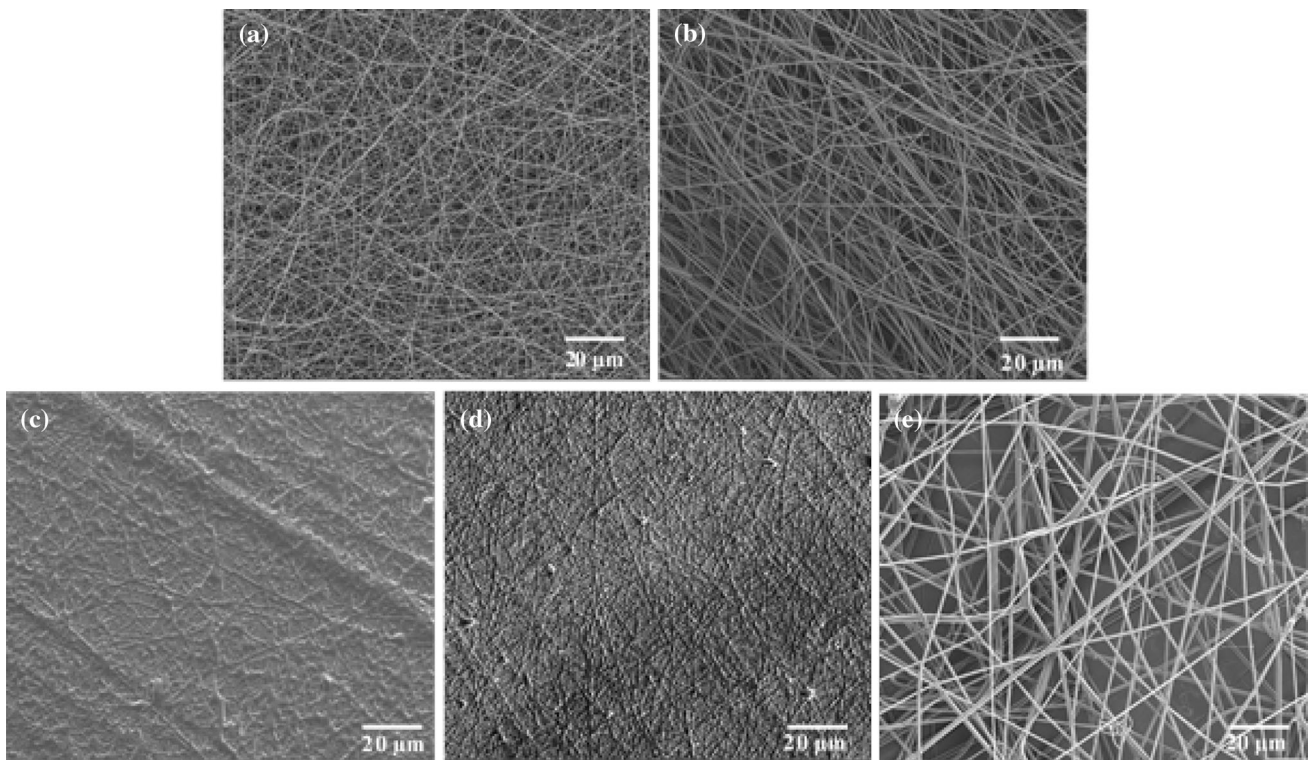
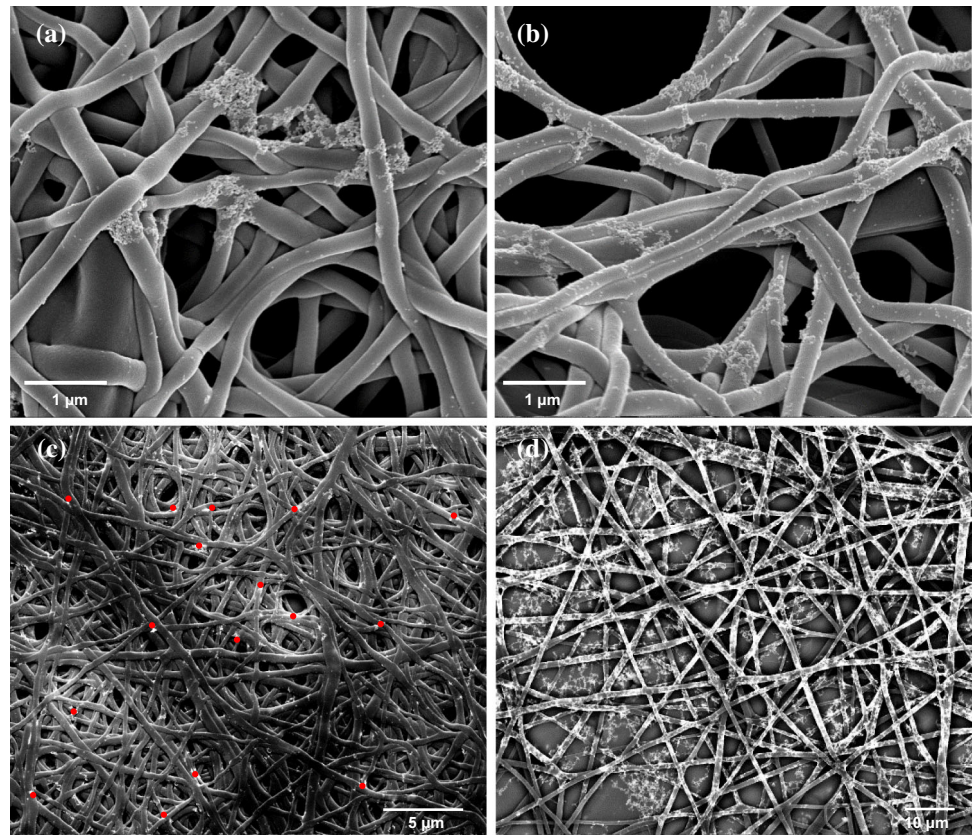


Figure 11 SEM images of uncrosslinked (a, c) and 12% crosslinked (b, d) zein nanofibers before (a, b) and after (c, d) water immersion for 30 min. Morphology of 12% crosslinked zein nanofibers after 8 months of storage in an uncontrolled relative humidity (e).

maintained their integrity and have almost unappreciable distortion and degradation. This is a good indicator of how these laboratory results when translated to a real manufacturing and storage environment would behave and the results are encouraging.

Atomic force microscopy

Nanofiber morphology can be clearly seen on the topography (uppermost layer) of fiber mats of both uncrosslinked and crosslinked fibers (Fig. 12a–b). The individual fiber contours are very visible and discernible on each AFM micrograph. In order to

make them clear and observable, contours have been drawn around individual fibers. In the uncrosslinked fiber mats, it is possible to visually observe that the fibers are more rounded and less densely packed; for the crosslinked zein fiber mats the individual fibers stand taller and are more densely packed which may be the outcome of the crosslinking of zein. At a surface area of $10\ \mu\text{m} \times 10\ \mu\text{m}$, the average surface roughness of the uncrosslinked nanofiber mats was calculated as 316.5 nm. The surface roughness is clearly linked to the contours of the fibers. At the same surface area, crosslinked zein nanofiber mats had a significantly higher surface roughness of 449.1 nm ($p < 0.05$) consistent with the observation

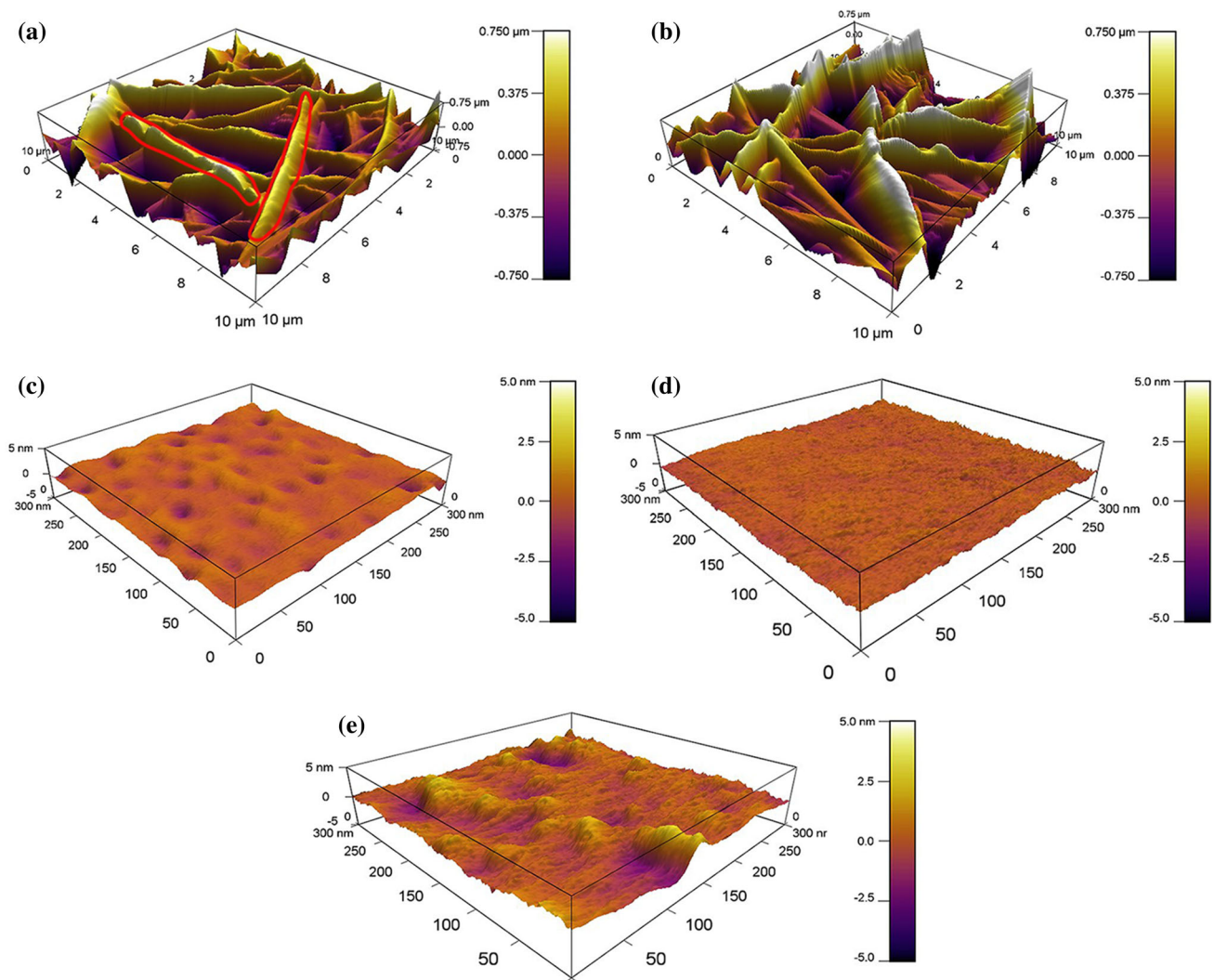


Figure 12 3D AFM images of zein nanofiber mats; **a** uncrosslinked zein nanofibers ($10\ \mu\text{m} \times 10\ \mu\text{m}$), **b** crosslinked zein nanofibers ($10\ \mu\text{m} \times 10\ \mu\text{m}$), **c** surface of single uncrosslinked zein nanofiber ($300\ \text{nm} \times 300\ \text{nm}$),

d surface of single crosslinked zein nanofiber ($300\ \text{nm} \times 300\ \text{nm}$), **e**: surface of Au nanoparticle-decorated crosslinked zein nanofiber ($300\ \text{nm} \times 300\ \text{nm}$). Red contours show single fibers in the mat.

that the fibers stand taller and are more densely packed.

When single fiber surfaces are studied, the roughness values were much lower. Uncrosslinked nanofibers had an average roughness value of 333.9 pm, and 12% crosslinked nanofibers had a roughness of 233.3 pm (Fig. 12c, d). The higher picometer-scale roughness on the uncrosslinked fibers may be a reflection of the higher porosity which results in rapid water absorption. The decrease in surface roughness with crosslinking on fiber surfaces may be the outcome of loss of porosity generated by the chemical crosslinking process. This results in a fiber unable to absorb water as rapidly as uncrosslinked zein fibers. The net relevant outcome is a higher degree of hydrophobicity to prevent the spreading of the water droplet, therefore concentrating gold nanoparticles to a much smaller area (Table 1). In addition, it is apparent from the micrographs that the micron-size roughness values increased with crosslinking, consistent with the changing surface wettability of the nanofiber mats. The micron-size roughness is larger for crosslinked zein fiber mats compared to the uncrosslinked fiber mats increasing the hydrophobicity of the surface by generating an effect similar to the lotus leaf effect. With gold nanoparticle-decorated crosslinked fibers, gold nanoparticles can also be clearly seen on the decorated nanofiber surface either as single nanoparticles or clustered nanoparticles (Fig. 12e). Gold nanoparticle decoration increased the average surface roughness of the crosslinked nanofibers to 712.7 pm.

Testing the zein nanofiber SERS platform

To test the effectiveness of the zein nanofiber platform, SERS experiments were conducted using Rhodamine 6G (R6G) as the Raman active molecule. Initially, different concentrations of R6G were tested on the zein nanofiber platforms, to determine the lowest concentration of R6G that can be used in the SERS experiments without any loss of peak information. All the operating parameters were kept constant while the effect of R6G concentration was studied. The concentrations tested were 1 mM, 100 μ M, 10 μ M and 1 μ M (Fig. 13). The R6G signature peaks at 616 cm^{-1} (C–C–C ring in plane bending), 776 cm^{-1} (C–C–C ring, out-of-plane bending), 1186 cm^{-1} (C–C stretching vibrations), 1365 cm^{-1} , 1513 cm^{-1} and 1654 cm^{-1} (aromatic) bands were

compared [26]. The spectra with 1 mM R6G had the most prominent peaks among all concentrations, as expected. These peaks are also present at 100 μ M concentration, but as expected they have lower intensities than 1-mM peaks. 10- μ M concentration spectra barely show any peaks, and almost no peaks were seen at 1 μ M R6G concentration. Based on these results, 100 μ M was chosen as the R6G concentration to be used in testing for the Raman enhancement.

To study the total SERS enhancement obtained with the crosslinked and uncrosslinked zein electrospun nanofiber platforms (with combined effects of Au nanoparticles and surface structure), the spectra of R6G on glass slide, on Au NP-decorated glass slide and on zein nanofiber sensor platform were compared (Fig. 14). For the measurement of R6G on glass slide, 100 mM R6G concentration was used, since lower concentrations of R6G did not show measurable peaks compared to the peaks obtained from the sensor platform. For R6G on Au NP-decorated glass slide and the zein-based sensor platforms, 100 μ M R6G was used. To increase the surface density of Au nanoparticle decoration on the surface of the fibers, crosslinked and uncrosslinked zein fiber mats were decorated with 3 Au colloid droplets. To clearly illustrate the SERS enhancement, the glass slide was also decorated with 3 droplets of Au NPs (see section “In-solution method” above).

0.1 M R6G on plain glass slide had the lowest Raman intensity, despite its much higher concentration, as expected based on prior studies since there are no gold nanoparticles present to enhance the signal [7]. When the glass slide was decorated with 3 consecutive Au nanoparticle droplets, a higher Raman signal was obtained from a lower R6G concentration (100 μ M). The Raman signal of R6G on uncrosslinked zein nanofiber platforms was slightly lower than R6G on Au nanoparticle-decorated glass slide. This is the result of the outward diffusion of gold nanoparticles to a wider area on the nanofiber mat due to its high hydrophilicity (Table 1). R6G on crosslinked zein nanofiber mats gave significantly higher Raman signals compared to uncrosslinked zein nanofiber mats because the increasing surface hydrophobicity resulting from crosslinking prevented spreading of Au nanoparticles to a wider area and increased the surface density AuNP and of hot spots.

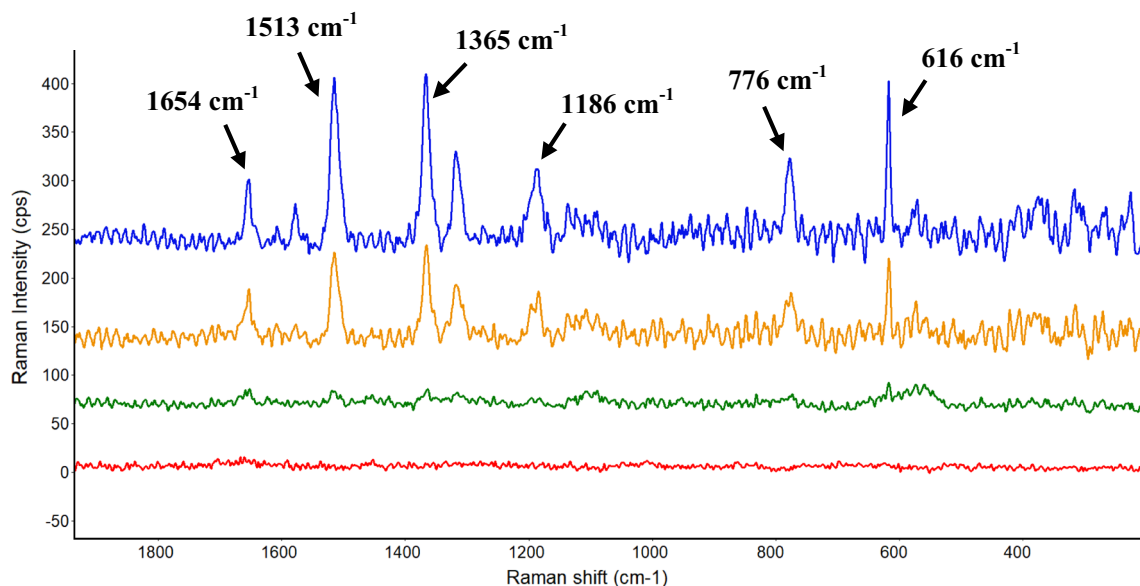


Figure 13 Raman spectra of Rhodamine 6G on zein nanofiber mats at different R6G concentrations; 1 μM (red), 10 μM (green), 100 μM (yellow) and 1 mM (blue).

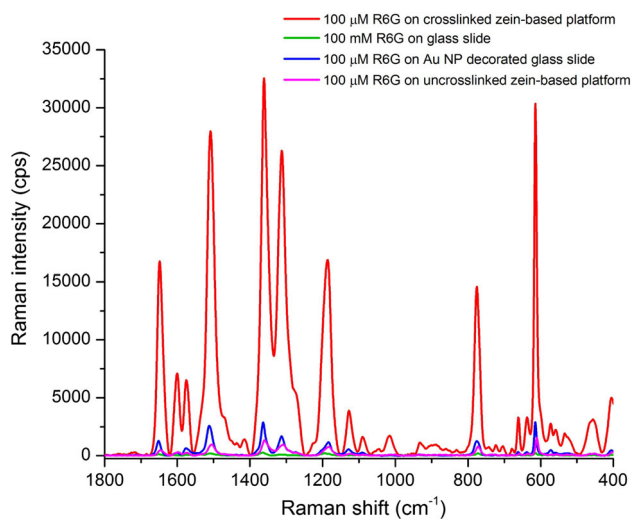


Figure 14 SERS enhancement of fabricated zein nanofiber platform. Red: spectrum of R6G on crosslinked zein nanofiber sensor platform (100 μM R6G), magenta: spectrum of R6G on uncrosslinked zein nanofiber sensor platform (100 μM R6G), blue: spectrum of R6G on Au nanoparticle-decorated glass slide (100 μM R6G), green: spectrum of R6G on glass slide (100 mM R6G).

For the calculation of total SERS enhancement, Eq. 1 is used and the intensities of R6G are compared based on the 1365-cm^{-1} peak [7].

$$\text{Enhancement Factor} = \frac{I_{\text{SERS}} \times N_{\text{Normal}}}{I_{\text{Normal}} \times N_{\text{SERS}}} \quad (1)$$

where I_{SERS} and I_{Normal} are the intensities obtained from SERS and non-SERS (normal) Raman experiments, while N_{SERS} and N_{Normal} are the number of R6G molecules contributing to these signals [27, 28]. To calculate the surface area covered with R6G on the glass slide was considered a flat circle ($d = 2.28 \pm 0.13$ mm), while for the surface area created by the zein nanofibers, the result of a prior study on electrospun zein nanofibers was adopted ($8.17 \text{ m}^2 \text{ g}^{-1}$) [11].

The total enhancement obtained from crosslinked AuNP decorated zein nanofiber sensor platform is calculated to be 1.06×10^6 . The enhancement factor of uncrosslinked zein nanofiber mats, on the other hand, is 4.3×10^4 . These enhancements are obtained by depositing 2.8×10^{-7} g of Au nanoparticles on the surface on zein nanofiber platform. This new strategy appears to be an improvement over our previous strategies using soft lithography where the surface of the zein platform with nanophotonic structures was covered by a gold layer with a thickness of 200 nm and the reported enhancement factor was 1.3×10^4 [7]. The enhancement obtained with crosslinked electrospun zein nanofiber platform in this study is almost 100 times higher than zein film-based substrate while the amount of gold used is approximately 803 times less (the calculations are done on weight basis). In addition, the SERS enhancement factor obtained in this study is comparable to some of

the non-biodegradable disposable SERS sensor platforms in the literature [29, 30]. There are also higher SERS enhancement factors achieved with different SERS sensor platform designs, such as Au nanoparticle monolayer with ultrasmall nanogaps [31] or g-C₃N₄-intercalated graphene oxide membranes [32] in the literature; however, the biodegradable protein sensor platform fabricated in this study offers better sustainability.

The sensor platform fabricated in this study uses a significantly less amount of gold while increasing the SERS enhancement due to its higher the surface area. Less use of gold is also more advantageous from the biodegradability point of view. In addition, the electrospinning technique is easy to operate and is more rapid compared to soft lithography, which includes curing of PDMS and drying of zein films for days [7]. Also in the technique developed in this study, there is no requirement for a master mold preparation through etching, which requires a considerable amount of time, is challenging and can be expensive. Therefore, the zein nanofiber-based SERS sensor platform serves an excellent green alternative from the production and the biodegradability point of view.

Conclusions

This paper summarizes the development and optimization of a novel biodegradable zein (corn protein)-based SERS sensor platform. To obtain a good SERS intensity and enhancement factor, the zein-based sensor platform was formed from zein nanofibers using electrospinning, which provides a very high surface area and surface roughness, the two key elements in increasing SERS intensity. Acetic acid was chosen as the better solvent relative to 70% ethanol for forming zein nanofibers, and the optimum zein concentration was found as 26 wt%, which yielded an average nanofiber diameter of 289 nm. Among the two gold nanoparticle decoration techniques, drop deposition technique gave a better surface coverage, with the limitation that it caused a slight fiber swelling (305 nm). 12% glutaraldehyde crosslinking prevented the swelling of zein nanofibers and increased the surface wettability, which also prevented the spreading diffusion of the gold nanoparticles through the fiber mat and increased hot spot formation. SERS measurements of Rhodamine

6G, a marker molecule, gave an enhancement factor of 1.06×10^6 , which is 100 times higher than the reported enhancement factor of a previously developed zein-based SERS sensor, by using 803 times less gold (by weight) [7]. The enhancement factor obtained is comparable if not somewhat superior to the plastic-based SERS sensor platforms while offering a largely eco-friendly, green alternative.

Acknowledgements

This research was supported with USDA Hatch funds and the Scholle Endowment funds. We also would like to thank Dr. Christopher Gilpin for his help with EDX and SEM imaging of the samples with backscattered electron detector.

Compliance with ethical standards

Conflict of interest The authors declare no conflict of interest with respect to the content of this study.

Electronic supplementary material: The online version of this article (<https://doi.org/10.1007/s10853-019-03504-w>) contains supplementary material, which is available to authorized users.

References

- [1] Thakur MS, Ragavan KV (2013) Biosensors in food processing. *J Food Sci Technol* 50:625–641. <https://doi.org/10.1007/s13197-012-0783-z>
- [2] Lawal AT (2016) Synthesis and utilization of carbon nanotubes for fabrication of electrochemical biosensors. *Mater Res Bull* 73:308–350. <https://doi.org/10.1016/j.materresbull.2015.08.037>
- [3] Maduraiveeran G, Sasidharan M, Ganesan V (2018) Electrochemical sensor and biosensor platforms based on advanced nanomaterials for biological and biomedical applications. *Biosens Bioelectron* 103:113–129. <https://doi.org/10.1016/j.bios.2017.12.031>
- [4] Tiwari JN, Vij V, Kemp KC, Kim KS (2016) Engineered carbon-nanomaterial-based electrochemical sensors for biomolecules. *ACS Nano* 10:46–80. <https://doi.org/10.1021/acsnano.5b05690>
- [5] Ding S-Y, Zhang X-M, Ren B, Tian Z-Q (2006) Surface-enhanced Raman spectroscopy (SERS): general introduction. In: *Encyclopedia of analytical chemistry*. Wiley, London

- [6] Shan C, Yang H, Han D et al (2010) Graphene/AuNPs/chitosan nanocomposites film for glucose biosensing. *Biosens Bioelectron* 25:1070–1074. <https://doi.org/10.1016/j.bios.2009.09.024>
- [7] Gezer PG, Hsiao A, Kokini JL, Liu GL (2016) Simultaneous transfer of noble metals and three-dimensional micro- and nanopatterns onto zein for fabrication of nanophotonic platforms. *J Mater Sci* 51:3806–3816. <https://doi.org/10.1007/s10853-015-9699-0>
- [8] Shan D, Li Q-B, Ding S-N et al (2010) Reagentless biosensor for hydrogen peroxide based on self-assembled films of horseradish peroxidase/laponite/chitosan and the primary investigation on the inhibitory effect by sulfide. *Biosens Bioelectron* 26:536–541. <https://doi.org/10.1016/j.bios.2010.07.051>
- [9] Zhao W, Yalcin B, Cakmak M (2015) Dynamic assembly of electrically conductive PEDOT:PSS nanofibers in electrospinning process studied by high speed video. *Synth Met* 203:107–116. <https://doi.org/10.1016/j.synthmet.2015.02.018>
- [10] Yan H, Mahanta NK, Wang B et al (2014) Structural evolution in graphitization of nanofibers and mats from electrospun polyimide–mesophase pitch blends. *Carbon* 71:303–318. <https://doi.org/10.1016/j.carbon.2014.01.057>
- [11] Brahatheeswaran D, Mathew A, Aswathy RG et al (2012) Hybrid fluorescent curcumin loaded zein electrospun nanofibrous scaffold for biomedical applications. *Biomed Mater* 7:045001. <https://doi.org/10.1088/1748-6041/7/4/045001>
- [12] Li Y, Li J, Xia Q et al (2012) Understanding the dissolution of alpha-zein in aqueous ethanol and acetic acid solutions. *J Phys Chem B* 116:12057–12064. <https://doi.org/10.1021/jp305709y>
- [13] Neo YP, Ray S, Eastal AJ et al (2012) Influence of solution and processing parameters towards the fabrication of electrospun zein fibers with sub-micron diameter. *J Food Eng* 109:645–651. <https://doi.org/10.1016/j.jfoodeng.2011.11.032>
- [14] Selling GW, Biswas A, Patel A et al (2007) Impact of solvent on electrospinning of zein and analysis of resulting fibers. *Macromol Chem Phys* 208:1002–1010. <https://doi.org/10.1002/macp.200700056>
- [15] Zhang H, Xi S, Han Y et al (2018) Determining electrospun morphology from the properties of protein–polymer solutions. *Soft Matter* 14:3455–3462. <https://doi.org/10.1039/C7SM02203D>
- [16] Turasan H, Barber EA, Malm M, Kokini JL (2018) Mechanical and spectroscopic characterization of cross-linked zein films cast from solutions of acetic acid leading to a new mechanism for the crosslinking of oleic acid plasticized zein films. *Food Res Int* 108:357–367. <https://doi.org/10.1016/j.foodres.2018.03.063>
- [17] Selling GW, Woods KK, Sessa D, Biswas A (2008) Electrospun zein fibers using glutaraldehyde as the crosslinking reagent: effect of time and temperature. *Macromol Chem Phys* 209:1003–1011. <https://doi.org/10.1002/macp.200700606>
- [18] Turasan H, Kokini JL (2017) Advances in understanding the molecular structures and functionalities of biodegradable zein-based materials using spectroscopic techniques: a review. *Biomacromol* 18:331–354. <https://doi.org/10.1021/acs.biomac.6b01455>
- [19] Shenoy SL, Bates WD, Frisch HL, Wnek GE (2005) Role of chain entanglements on fiber formation during electrospinning of polymer solutions: good solvent, non-specific polymer–polymer interaction limit. *Polymer* 46:3372–3384. <https://doi.org/10.1016/j.polymer.2005.03.011>
- [20] Yao C, Li X, Song T (2007) Electrospinning and crosslinking of zein nanofiber mats. *J Appl Polym Sci* 103:380–385. <https://doi.org/10.1002/app.24619>
- [21] Vogt L, Liverani L, Roether JA, Boccaccini AR (2018) Electrospun zein fibers incorporating poly(glycerol sebacate) for soft tissue engineering. *Nanomaterials* 8:150. <https://doi.org/10.3390/nano8030150>
- [22] Ma M, Hill RM (2006) Superhydrophobic surfaces. *Curr Opin Colloid Interface Sci* 11:193–202. <https://doi.org/10.1016/j.cocis.2006.06.002>
- [23] Ma M, Mao Y, Gupta M et al (2005) Superhydrophobic fabrics produced by electrospinning and chemical vapor deposition. *Macromolecules* 38:9742–9748. <https://doi.org/10.1021/ma0511189>
- [24] Singh A, Steely L, Allcock HR (2005) Poly[bis(2,2,2-trifluoroethoxy)phosphazene] superhydrophobic nanofibers. *Langmuir* 21:11604–11607. <https://doi.org/10.1021/la052110v>
- [25] Cheng YT, Rodak DE, Wong CA, Hayden CA (2006) Effects of micro- and nano-structures on the self-cleaning behaviour of lotus leaves. *Nanotechnology* 17:1359. <https://doi.org/10.1088/0957-4484/17/5/032>
- [26] Pristiniski D, Tan S, Erol M et al (2006) In situ SERS study of Rhodamine 6G adsorbed on individually immobilized Ag nanoparticles. *J Raman Spectrosc* 37:762–770. <https://doi.org/10.1002/jrs.1496>
- [27] Chang T-W, Gartia MR, Seo S et al (2014) A wafer-scale backplane-assisted resonating nanoantenna array SERS device created by tunable thermal dewetting nanofabrication. *Nanotechnology* 25:145304. <https://doi.org/10.1088/0957-4484/25/14/145304>
- [28] Liu Y, Xu S, Li H et al (2011) Localized and propagating surface plasmon co-enhanced Raman spectroscopy based on

- evanescent field excitation. *Chem Commun* 47:3784–3786. <https://doi.org/10.1039/C0CC04988C>
- [29] Zhai W-L, Li D-W, Qu L-L et al (2012) Multiple depositions of Ag nanoparticles on chemically modified agarose films for surface-enhanced Raman spectroscopy. *Nanoscale* 4:137–142. <https://doi.org/10.1039/C1NR10956A>
- [30] Qu L-L, Li D-W, Xue J-Q et al (2012) Batch fabrication of disposable screen printed SERS arrays. *Lab Chip* 12:876–881. <https://doi.org/10.1039/C2LC20926H>
- [31] Si S, Liang W, Sun Y et al (2016) Facile fabrication of high-density sub-1-nm gaps from Au nanoparticle monolayers as reproducible SERS substrates. *Adv Funct Mater* 26:8137–8145. <https://doi.org/10.1002/adfm.201602337>
- [32] Qu L, Wang N, Xu H et al (2017) Gold nanoparticles and g-C₃N₄-intercalated graphene oxide membrane for recyclable surface enhanced Raman scattering. *Adv Funct Mater* 27:1701714. <https://doi.org/10.1002/adfm.201701714>

Publisher's Note Springer Nature remains neutral with regard to jurisdictional claims in published maps and institutional affiliations.